ACS Medicinal Chemistry Letters

Letter

Cite This: ACS Med. Chem. Lett. 2017, 8, 1194-1198

pubs.acs.org/acsmedchemlett

Benzoxaboroles as Efficient Inhibitors of the β-Carbonic Anhydrases from Pathogenic Fungi: Activity and Modeling Study

Alessio Nocentini,[†,‡] Roberta Cadoni,[†] Sonia del Prete,[§] Clemente Capasso,[§] Pascal Dumy,[†] Paola Gratteri,[‡] Claudiu T. Supuran,*[,#] and Jean-Yves Winum*[,†]

[†]Institut des Biomolécules Max Mousseron (IBMM), UMR 5247 CNRS, ENSCM, Université de Montpellier, 240 avenue du Professeur Emile Jeanbrau, 34296 Montpellier Cedex 05, France

[‡]Department of NEUROFARBA, Section of Pharmaceutical and Nutraceutical Sciences, Laboratory of Molecular Modeling Cheminformatics & QSAR, University of Florence, Polo Scientifico, Via U. Schiff 6, 50019 Sesto Fiorentino (Firenze), Italy

[§]Istituto di Bioscienze e Biorisorse, CNR, Via Pietro Castellino 111, 80131 Napoli, Italy

[#]Department of NEUROFARBA, Section of Pharmaceutical and Nutraceutical Sciences, University of Florence, Polo Scientifico, Via U. Schiff 6, 50019 Sesto Fiorentino (Firenze), Italy

Supporting Information

ABSTRACT: A series of 6-substituted benzoxaboroles were investigated as inhibitors of the β-class carbonic anhydrase from three pathogenic fungi (*Cryptococcus neoformans*, *Candida glabrata*, and *Malassezia globosa*). Independently from the nature of the substituents on the phenyl of the urea/thiourea group, all reported derivatives showed nanomolar inhibitory activities against Can2 and CgNce103 vs micromolar inhibition against MgCA. Selectivity over human CA I and CA II was noticed. The observed structure−activity relationship trends have been rationalized by modeling study of selected compounds into the active site of Can2 and MgCA. The present letter demonstrates that benzoxaborole chemotype may offer interesting opportunities for the inhibition of β-CA from pathogenic fungi and for the development of antifungal agents with a new mechanism of action.

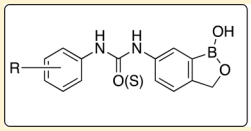

nanomolar inhibitor of β-CAs from *Cryptococcus neoformans* (Can2) and *Candida Glabrata* (CgNce103)

micromolar inhibitor of β-CAs from *Malassezia globosa* (MgCA)

KEYWORDS: *Carbonic anhydrase, β-CA-class enzyme, benzoxaborole, inhibitor, Malassezia globosa, Cryptococcus neoformans, Candida albicans*

Carbonic anhydrases (CAs, EC.4.2.1.1) are ubiquitous zinc metalloproteins, found in most eukaryotic and prokaryotic organisms, which catalyze efficiently the reversible hydration of carbon dioxide to bicarbonate with release of a proton.[1] Due to their involvement in several biosynthetic and pathological processes, several isoforms from the human α-CA have been extensively studied as potential targets for therapeutic intervention, for example, in glaucoma and, recently, in cancer.[2,3]

The potential of carbonic anhydrases as anti-infective targets has also been taken in consideration recently, and prokaryotic carbonic anhydrases from different classes were proposed as new promising targets in the search of novel agents (antibiotics, antifungals and antiprotozoans) that lack cross-resistance to existing drugs.[4−6]

The inhibitory profile of most of the important classes of CAIs against β-CA, sulfonamides and bioisosteres, inorganic anions, and carboxylate, have been investigated in detail.[7] Recently, new chemotypes, such as phenol and dithiocarbamate, were also reported as efficient fungal β-CA inhibitors.[8,9] However, one of the main drawbacks of the previous screening data was related to the selectivity. Even if compounds with high selectivity against specific α-CA isoforms have been reported, the main challenge always remaining is the selectivity for the inhibition of β- over α-CA.[10]

In the context of structure-based drug design campaigns, an under explored nonsulfonamide class of inhibitors emerged in the last years. Proposed in 2009 by our groups, boron containing inhibitors (boronic acid) were investigated as potential α-CA from human and β-CA from pathogenic fungi.[11,12] These first studies allowed to consider boronic acid function as new zinc binding group for the design of effective inhibitors.[13]

In 2016, two studies reported the activity of the boronic acid peptidomimetic bortezomib against mammalian α-CA and prokaryotic β-CA.[14,15] Bortezomib, a marketed proteasome inhibitor, exhibited an inhibitory profile in the micromolar range against mammalian α-CA but also against β-CA from pathogenic fungi and bacteria.

In order to expand molecular diversity, we reported in 2016, a new generation of α-class carbonic anhydrase inhibitors using the benzoxaborole scaffold as an attractive alternative chemotype having a completely new binding mode to the α-CA active site.[16] The attractive features offered by benzoxaborole heterocycle[17] allowed us to modify the substitution pattern on position 6, showing the possibility to modulate the affinity

Received: September 7, 2017
Accepted: October 20, 2017
Published: October 20, 2017

DOI: 10.1021/acsmedchemlett.7b00369
ACS Med. Chem. Lett. 2017, 8, 1194−1198

and the binding mode toward the different CA isoforms, reaching for some derivatives nanomolar inhibitory activities.

In this letter, we report nanomolar inhibitory activities and computational studies of a series of benzoxaboroles as well as Tavaborole (a benzoxaborole derivatives marketed under the trade name Kerydin and used in clinic for the topical treatment of fungal nail infection known as onychomycosis) against β-CA from three pathogenic fungi (*Cryptococcus neoformans* (Can2), *Malassezia globosa* (MgCA), and *Candida glabrata* (CgNce103).[14]

The benzoxaborole series investigated in this study was prepared as previously reported by reaction of 6-amino-benzoxaborole with different iso- or isothiocyanate.[16]

Inhibition data with benzoxaboroles **1**−**23** against pathogenic fungi CAs and hCA off-targets (hCA I and hCA II) are shown in Table 1. Sulfonamide inhibitor acetazolamide was used as a standard as well as Tavaborole. The displayed inhibitory activities were compared to the ones previously reported against the off-target widely-distributed human h isoforms hCA I and hCA II.[16]

The following SAR for the inhibitory properties of **1**−**23** (Table 1) indicates that changes in the substitution pattern on the phenyl ring of the ureido/thioureido group lead to differences of the inhibitory activity and selectivity vs hCA I and hCA II. At the same time, changing ureido by a thioureido group did not affect significantly inhibition.

All benzoxaboroles (**1**−**23**, Chart 1) were much more effective inhibitors against Can2 and CgNce β-CA than against MgCA with respectively nanomolar vs micromolar potency. Moreover these inhibitors **1**−**23** were slightly more selective on Can2 and CgNce103 β-CA over human α-CA off-targets hCA I and hCA II. The most notable example is provided by compound **18**, which demonstrated the best selectivity against fungal CA with a selectivity ratio compared to hCA II superior to 100 (K_I hCA II/K_I Can2 > 127 and K_I hCA II/K_I CgNce >103). This compound is in fact the most selective benzoxaborole inhibitor detected so far for Can 2.

Substitution of the phenyl ring of the urea/thiourea group had diverse effects on the inhibitory power of the benzoxaboroles. Against Can2, nanomolar activities ranging from 65 to 676 nM were observed, the best inhibitor being the acetyl derivatives **13**. Against CgNCe103, benzoxaboroles were also nanomolar inhibitors with K_I between 75 and 467 nM, the best being compound **9**. In fact, the differences of inhibition constants were not very important when comparing inhibition profile against Can2 and CgNce103.

Benzoxaboroles **1**−**23** did not exhibit better activity on Can2 and CgNce β-CA compared to the clinically used sulfonamide drug acetazolamide (K_I of 10−11 nM), with inhibition constants ranging between 383 and 6235 nM. Against MgCA, inhibitory activities of **1**−**23** were comparable with those of acetazolamide. The only exceptions were represented by derivatives **18** and **19** with activities roughly ten times better (respectively K_I of 8.6 and 5.3 μM).

Except the nonsubstituted compound **1**, all the reported benzoxaboroles displayed a better efficacy in inhibiting MgCA compared to the clinically used benzoxaborole drug tavaborole (K_I of 99 μM), with K_Is spanning between 5 and 98 μM. Against Can2 and CgNce β-CA, Tavaborole displayed inhibitory activity (K_I respectively of 89 and 72 nM) in the same nanomolar range as the best inhibitors **6**, **7**, **9**, **11**, **17**, **18**, and **20.** Important information to note is the inhibition profile of Tavaborole against human hCA I and hCA II, which is roughly identical with the 6-substituted benzoxaborole **2** and **3**, inhibitory activity being always better against hCA II vs hCA I.

Molecular modeling investigations were undertaken to investigate in-depth the interesting inhibitory profiles of the benzoxaboroles against the β-CAs from *Malassezia globosa* (MgCA) and *Cryptococcus neoformans* (Can2).

Table 1. Inhibition Data of hCA I, hCA II, and β-CA Isoforms, MgCA, Can2, and CgNce103, with Benzoxaboroles 1−23 and Tavaborole and the Standard Sulfonamide Inhibitor Acetazolamide by a Stopped Flow CO_2 Hydrase Assay

		K_I (nM)[a]				
		MgCA	Can2	CgNce	hCA I	hCA II
1	H	109130	174	260	5690	8180
2	NO_2	91276	88	89	6352	504
3	NH_2	44603	93	244	9435	590
4	NHCONH−CH_2Ph	58214	602	201	557	439
5	NHCONH−CH_2−(3-Cl,5-CH_3-Ph)	86833	400	79	570	276
6	NHCONH−Ph	63687	81	86	654	730
7	NHCONH−(4-Cl-Ph)	77855	92	81	3465	707
8	NHCONH−CH_2−fur-2-yl	55637	283	96	613	841
9	NHCONH−(4-F-Ph)	76193	78	75	235	480
10	NHCONH−(4-CF_3−Ph)	73614	84	96	487	456
11	NHCONH−(2,4,6-Cl-Ph)	98557	73	81	450	272
12	NHCONH−(2-OMe,5-CH_3-Ph)	71221	248	78	98	89
13	NHCONH−(4-$COCH_3$-Ph)	62187	65	203	288	797
14	NHCSNH−CH_2CH_2Ph	22531	676	467	639	1547
15	NHCSNH−(4-CH_3-Ph)	24906	181	89	318	1253
16	NHCSNH−napht-2-yl	30625	573	339	548	1148
17	NHCSNH−(4-OCH_3−Ph)	28765	89	86	514	1250
18	NHCSNH−(4-NO_2−Ph)	8675	79	96	385	>10000
19	NHCSNH−CH_2Ph	5346	537	334	380	1305
20	NHCSNH−(4-F-Ph)	30100	86	86	355	1500
21	NHCSNH−CH_2−fur-2-yl	6095	236	229	258	2230
22	NHCSNH−(4-CF_3−Ph)	49762	275	112	417	1838
23	NHCSNH-Ph	21319	198	97	532	1625
tavaborole		99022	89	72	2015	462
acetazolamide		76000	10	11	250	12

[a]Mean from three different assays, by a stopped flow technique (errors were in the range of ±5−10% of the reported values).

Chart 1. Structure of Benzoxaborole 1−23, Tavaborole, and Acetazolamide

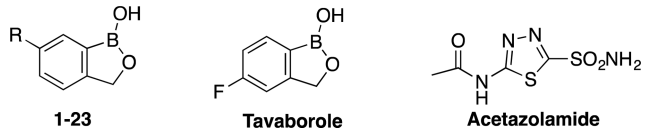

DOI: 10.1021/acsmedchemlett.7b00369
ACS Med. Chem. Lett. 2017, 8, 1194−1198

Table 2. Non-conserved Residues in MgCA and Can2 within 6 Å from the Benzoxaborole Core

MgCA	Can2
A:S84	A:A105
A:T87	A:N108
A:F88	A:Y109
A:A92	A:N113
A:L93	A:V114
B:S48	B:A69
B:S105	B:G126
B:V109	B:C130
B:A110	B:I131
B:H135	B:Y152

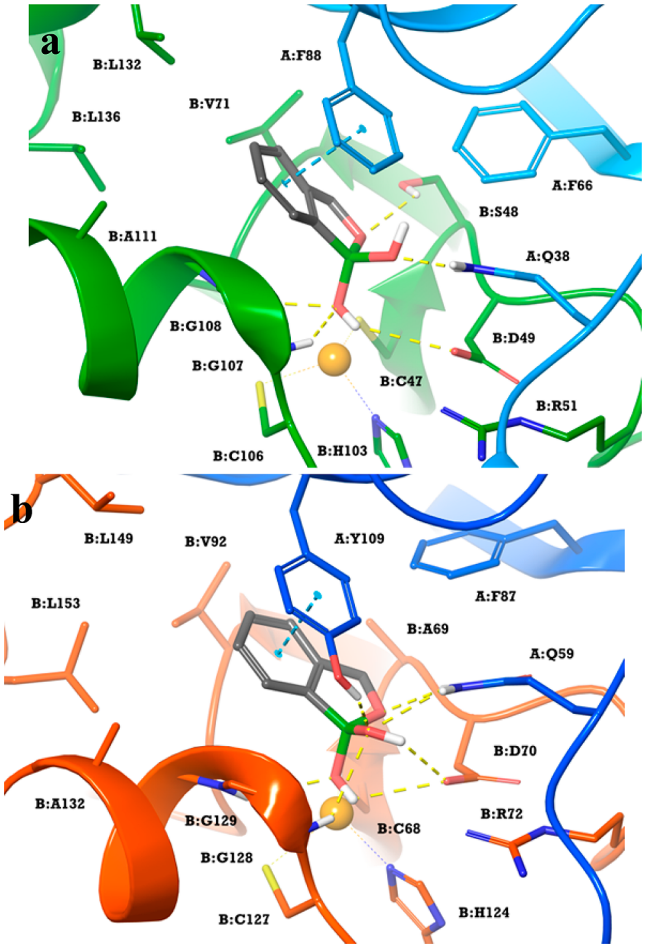

Figure 1. Docking orientations of benzoxaborole within (a) MgCA and (b) Can2 active sites. Monomers A and B are colored light blue and green (MgCA) and blue and orange (Can2), respectively. H-bonds and $\pi-\pi$ interactions are highlighted by yellow and blue dashed lines, respectively.

A common feature of the studied compounds is the presence of the benzoxaborole core functionalized in position 6 by groups with different size and chemical properties. As the tetrahedral anionic form of benzoxaboroles was found to coordinate the hCA II zinc ion,[16] the charged hydroxylated (e.g., $B(OH)_2^-$) forms of some representative derivatives in Table 1 were submitted to QM geometry optimization (B3LYP/6-31G*$^+$), and ESP charges were computed prior to docking the molecules into the recently developed homology-built model of MgCA[9] and into the X-ray solved structure of

Table 3. Hydrogen Bonds between Benzoxaborole and β-CA Isoforms MgCA and Can2

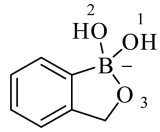

MgCA		Can2	
atoms	d(H···A) (Å)	atoms	d(H···A) (Å)
O1···HN B:G107	2.3	O1···HN B:G129	2.8
O1···HN B:G108	2.8	O1−H···OD B:D70	2.8
O1−H···OD B:D49	3.1	O2···HH B:Y109	2.2
O2···HE A:Q38	2.1	O2···HN B:G128	2.8
O3···HG B:S48	2.5	O2···HE A:Q59	2.7
		O2−H···OD B:D70	2.4
		O2···HA B:G128	2.9
		O3···HE A:Q59	2.3

Can2 (PDB 2W3N).[18] The active pockets of these enzymes comprise residues from the two monomers (chains A and B) and share many common features, as well as some differences that modulate the inhibitory activities of the benzoxaboroles against the two fungal isoforms (Table 2).

Differently from the zinc-coordination geometries found in the X-ray structures of hCA II-benzoxaborole adducts, findings from docking within the MgCA and Can2 only revealed that the boron-bonded OH of derivatives in Table 1 occupied the fourth coordination position, so defining the tetrahedral coordination sphere of the Zn ion (Figure 1). The coordination environment of the catalytic metal ion is completed by the side chains of two cysteine residues and a histidine residue (i.e., MgCA with C47, H103, and C106; Can2 with C68, H124, and C127).

The tendency of inhibitory efficacy of derivatives in Table 1, two orders of magnitude greater for Can2 than MgCA, is likely to depend on the different network of H-bonds to which the anionic form of the boronic ester moiety takes part. This network includes, together with others, residues that are mutated in the two enzymes and in particular B:S48/A69 and A:F88/Y109 (Table 2). Within the MgCA binding site (Figure 1a) the Zn-coordinated OH group (O1 Table 3) was involved in three H-bonds, acting as a bifurcated acceptor in the interaction with the backbone NH of B:G107 and B:G108 and as donor with the OD of B:D49. The second hydroxyl group (O2 Table 3) was in H-bond distance with A:Q38 (O···HE), whereas the cyclic boronic ester oxygen accepts the HG hydrogen atom from the B:S48 side chain (Table 3). In addition to this set of interactions, the molecule is further stabilized by face to face $\pi-\pi$ and π−alkyl interactions occurring with the side chains of A:F88, B:V71, and B:L132.

The chemical features and the size of Can2 binding site is modified due to the two-residue mutation, causing a different position of the benzoxaborole scaffold if compared to what is observed in MgCA (Figure 1b). The Zn-coordinated OH group (O1 Table 3) mostly holds the same interactions described for the MgCA, whereas the second OH (O1 Table 3) is H-bonded to the B:D70 (OH···OD) to which it donates the proton while it accepts the HH and HE hydrogens from the B:Y109 and A:Q59, respectively. Additionally, it gives rise either to conventional and nonconventional H-bonds with B:G128. The A:Q59 side chain donates the hydrogen HE to the cyclic boronic ester oxygen (Table 3). The aromatic portion of the

DOI: 10.1021/acsmedchemlett.7b00369
ACS Med. Chem. Lett. 2017, 8, 1194−1198

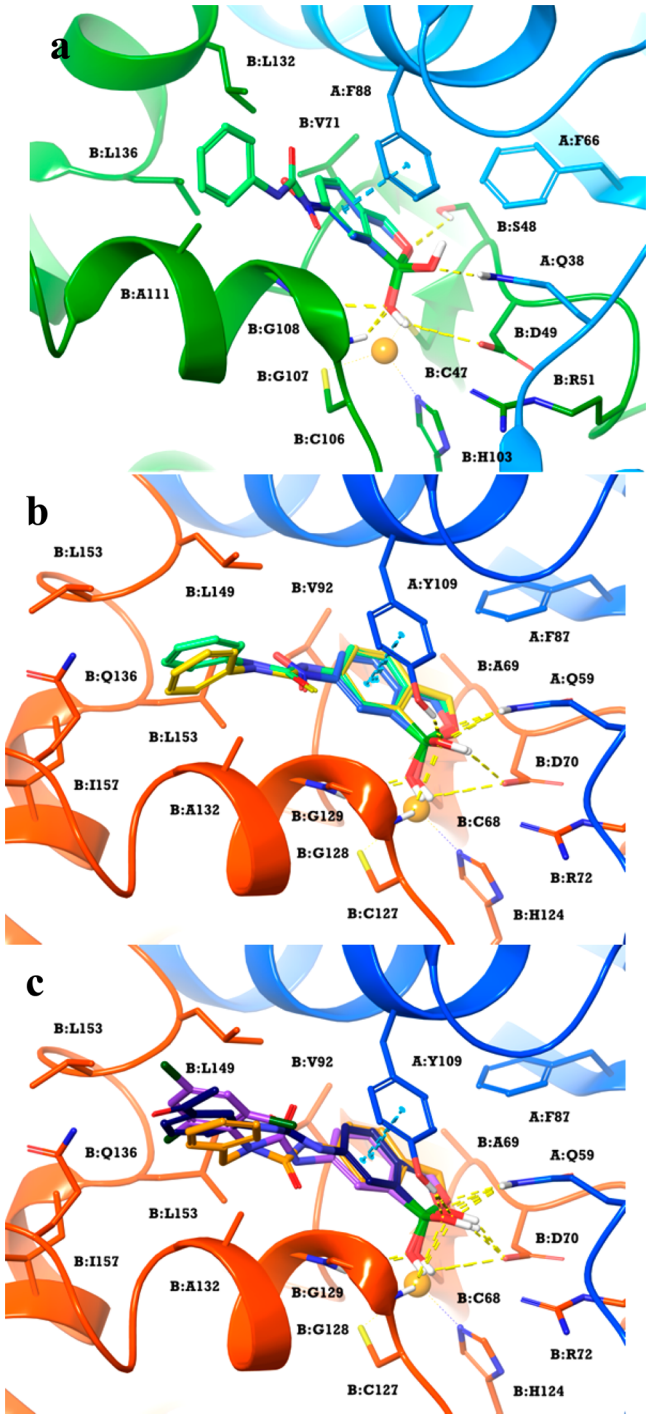

Figure 2. (a) Predicted binding modes of **2** (light blue) and **6** (green), within MgCA active site. The nitro group of **2** established lipophilic contacts with B:A111, B:L132, and B:G107. The ureido group of **6** was involved in a three-center H-bond with B:G107. Predicted binding modes of (b) **2** (light blue), **6** (green), **23** (yellow) and (c) **4** (orange), **11** (purple), **13** (blue) within CAN2 active site. Monomers A and B are colored light blue and green (MgCA) and blue and orange (Can2), respectively. H-bonds and $\pi-\pi$ interactions are highlighted, respectively, by yellow and blue dashed lines.

ligand is sandwiched between the hydrophobic surface of B:Y109 on one side and B:V92 on the other, establishing $\pi-\pi$ and π−alkyl contacts.

The set of interactions described above applies to the benzoxaborole core of all the studied derivatives. Results from

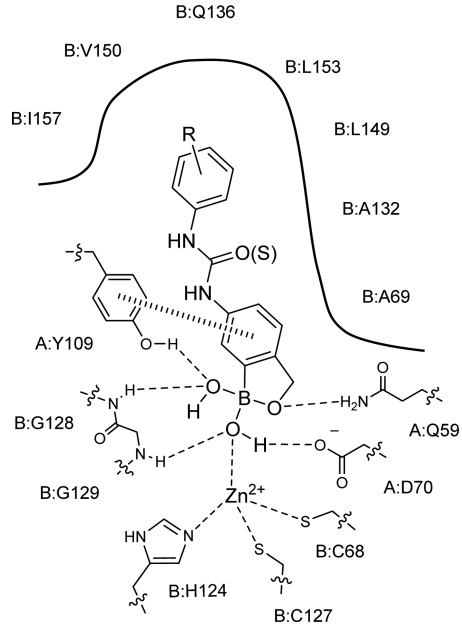

Figure 3. Schematic representation of the binding mode of 6-substituted benzoxaboroles in the Can2 active site.

docking within MgCA indicate that the pendants at position 6 point out toward the outer part of the binding site, and all give rise to almost the same kind of interactions with the residues of the enzymatic counterpart (Figure 2a). This is consistent with the inhibitory profile of derivatives in Table 1 that, as a matter of fact, do not vary considerably throughout the set of the synthesized compounds.

Conversely, because of the orientations adopted by the benzoxaborole scaffold within Can2, the substituents in position 6 accommodate an area lined by the residues A132, Q136, L149, V150, L153, I157, all belonging to the chain B (Figures 2b,c and 3). The NO_2 and NH_2 groups of derivatives **2** and **3**, as well as Tavaborole, face this hydrophobic cleft (Figure 3). Instead, the aryl ureido/thioureido moieties of the remaining derivatives more deeply accommodate the hydrophobic pocket, and their aromatic portions establish extensive van der Waals interactions with the surrounding residues (Figures 2b,c and 3). Within this pocket **13** positions its acetyl group at a hydrogen bond distance from B:Q136. Due to the presence in **4** of the CH_2 spacer between the urea and the aromatic tail, the position of this latter slightly differs from that of the other derivatives, moving away from the hydrophobic pocket and thus losing stabilizing interactions (Figure 2c). The replacement of the urea oxygen with a sulfur atom did not substantially modify the pose assumed by the compounds.

We report here the first inhibition study of the β-CAs from three fungal pathogens with the benzoxaborole derivatives. The following pathogenic fungi *Cryptococcus neoformans*, *Candida glabrata*, and *Malassezia globosa* were included in the study. Benzoxaborole derivatives **1**−**23** were micromolar inhibitors against MgCA, displaying K_Is in the range 5.3−109 μM and nanomolar inhibitors against both CgNce β-CA and Can2. For some benzoxaborole derivatives, strong selectivity against Can2 vs the off-target hCA II was observed.

Based on a molecular modeling study, the comparison of structural features of the binding mode of benzoxaborole within the active site of Can2 or MgCA shows a correlation with the inhibitory activity. The residue mutation in the close proximity

DOI: 10.1021/acsmedchemlett.7b00369
ACS Med. Chem. Lett. 2017, 8, 1194−1198

of the binding site (6 Å) of both enzymes results in a different positioning of the benzoxaborole motif. Consequently, the hydrophobic pocket of Can2 CA binding site can easily accommodate the aryl ureido/thioureido moieties in position 6 of the benzoxaborole scaffold, whereas in the case of MgCA these substituents are pointing out toward the outer part of the binding site.

These results support that substituted benzoxaborole heterocycles are attractive chemotypes for further consideration in drug design and development of antifungals with a novel mechanism of action, based on selective fungal−CA inhibition.

■ ASSOCIATED CONTENT

Supporting Information

The Supporting Information is available free of charge on the ACS Publications website at DOI: 10.1021/acsmedchemlett.7b00369.

CA inhibition assay and molecular modeling (PDF)

■ AUTHOR INFORMATION

Corresponding Authors

*E-mail: claudiu.supuran@unifi.it.

*E-mail: jean-yves.winum@umontpellier.fr.

ORCID

Paola Gratteri: 0000-0002-9137-2509

Claudiu T. Supuran: 0000-0003-4262-0323

Jean-Yves Winum: 0000-0003-3197-3414

Author Contributions

The manuscript was written through contributions of all authors. All authors have given approval to the final version of the manuscript.

Notes

The authors declare no competing financial interest.

■ ACKNOWLEDGMENTS

We thank the LabEx CheMISyst (ANR-10-LABX-05-01) for funding.

■ ABBREVIATIONS

CA, carbonic anhydrase; MgCA, *Malassezia globosa* carbonic anhydrase; CgNce103, *Candida glabrata* carbonic anhydrase; Can2, *Cryptococcus neoformans* carbonic anhydrase

■ REFERENCES

(1) Supuran, C. T. Carbonic anhydrases: novel therapeutic applications for inhibitors and activators. *Nat. Rev. Drug Discovery* **2008**, *7*, 168−81.

(2) Scozzafava, A.; Supuran, C. T. Glaucoma and the applications of carbonic anhydrase inhibitors. *Subcell. Biochem.* **2014**, *75*, 349−59.

(3) Supuran, C. T.; Winum, J. Y. Carbonic anhydrase IX inhibitors in cancer therapy: an update. *Future Med. Chem.* **2015**, *7*, 1407−14.

(4) Capasso, C.; Supuran, C. T. Bacterial, fungal and protozoan carbonic anhydrases as drug targets. *Expert Opin. Ther. Targets* **2015**, *19*, 1689−704.

(5) Vermelho, A. B.; Capaci, G. R.; Rodrigues, I. A.; Cardoso, V. S.; Mazotto, A. M.; Supuran, C. T. Carbonic anhydrases from Trypanosoma and Leishmania as anti-protozoan drug targets. *Bioorg. Med. Chem.* **2017**, *25*, 1543−1555.

(6) Capasso, C.; Supuran, C. T. Inhibition of Bacterial Carbonic Anhydrases as a Novel Approach to Escape Drug Resistance. *Curr. Top. Med. Chem.* **2017**, *17*, 1237−1248.

(7) Supuran, C. T. Advances in structure-based drug discovery of carbonic anhydrase inhibitors. *Expert Opin. Drug Discovery* **2017**, *12*, 61−88.

(8) Karioti, A.; Carta, F.; Supuran, C. T. Phenols and Polyphenols as Carbonic Anhydrase Inhibitors. *Molecules* **2016**, *21*, 1649.

(9) Vullo, D.; Del Prete, S.; Nocentini, A.; Osman, S. M.; AlOthman, Z.; Capasso, C.; Bozdag, M.; Carta, F.; Gratteri, P.; Supuran, C. T. Dithiocarbamates effectively inhibit the β-carbonic anhydrase from the dandruff-producing fungus *Malassezia globosa*. *Bioorg. Med. Chem.* **2017**, *25*, 1260−1265.

(10) Capasso, C.; Supuran, C. T. An Overview of the Selectivity and Efficiency of the Bacterial Carbonic Anhydrase Inhibitors. *Curr. Med. Chem.* **2015**, *22*, 2130−9.

(11) Winum, J. Y.; Innocenti, A.; Scozzafava, A.; Montero, J. L.; Supuran, C. T. Carbonic anhydrase inhibitors. Inhibition of the human cytosolic isoforms I and II and transmembrane, tumor-associated isoforms IX and XII with boronic acids. *Bioorg. Med. Chem.* **2009**, *17*, 3649−52.

(12) Innocenti, A.; Winum, J. Y.; Hall, R. A.; Mühlschlegel, F. A.; Scozzafava, A.; Supuran, C. T. Carbonic anhydrase inhibitors. Inhibition of the fungal beta-carbonic anhydrases from *Candida albicans* and *Cryptococcus neoformans* with boronic acids. *Bioorg. Med. Chem. Lett.* **2009**, *19*, 2642−5.

(13) Winum, J. Y.; Supuran, C. T. Recent advances in the discovery of zinc-binding motifs for the development of carbonic anhydrase inhibitors. *J. Enzyme Inhib. Med. Chem.* **2015**, *30*, 321−4.

(14) Supuran, C. T. Bortezomib inhibits mammalian carbonic anhydrases. *Bioorg. Med. Chem.* **2017**, *25*, 5064−67.

(15) Supuran, C. T. Bortezomib inhibits bacterial and fungal β-carbonic anhydrases. *Bioorg. Med. Chem.* **2016**, *24*, 4406−9.

(16) Alterio, V.; Cadoni, R.; Esposito, D.; Vullo, D.; Fiore, A. D.; Monti, S. M.; Caporale, A.; Ruvo, M.; Sechi, M.; Dumy, P.; Supuran, C. T.; De Simone, G.; Winum, J. Y. Benzoxaborole as a new chemotype for carbonic anhydrase inhibition. *Chem. Commun.* **2016**, *52*, 11983−11986.

(17) Adamczyk-Woźniak, A.; Borys, K. M.; Sporzyński, A. Recent Developments in the Chemistry and Biological Applications of Benzoxaboroles. *Chem. Rev.* **2015**, *115*, 5224−5247.

(18) Schlicker, C.; Hall, R. A.; Vullo, D.; Middelhaufe, S.; Gertz, M.; Supuran, C. T.; Muehlschlegel, F. A.; Steegborn, C. Structure and Inhibition of the CO_2-Sensing Carbonic Anhydrase Can2 from the Pathogenic Fungus *Cryptococcus neoformans*. *J. Mol. Biol.* **2009**, *385*, 1207−1220.

DOI: 10.1021/acsmedchemlett.7b00369
ACS Med. Chem. Lett. 2017, 8, 1194−1198